

# Direct Evidence for the Cooperative Unfolding of Cytochrome *c* in Lipid Membranes from H-<sup>2</sup>H Exchange Kinetics

Teresa J. T. Pinheiro<sup>1\*</sup>, Hong Cheng<sup>2</sup>, Steven H. Seeholzer<sup>2</sup> and Heinrich Roder<sup>2,3</sup>

<sup>1</sup>*Department of Biological Sciences, University of Warwick, Gibbet Hill Road Coventry CV4 7AL, UK*

<sup>2</sup>*Institute for Cancer Research Fox Chase Cancer Center, 7701 Burholme Avenue, Philadelphia PA, 19111, USA*

<sup>3</sup>*Department of Biochemistry & Biophysics, University of Pennsylvania, Philadelphia PA 19104, USA*

The interaction of cytochrome *c* (cyt *c*) with anionic lipid membranes is known to disrupt the tightly packed native structure of the protein. This process leads to a lipid-inserted denatured state, which retains a native-like  $\alpha$ -helical structure but lacks any specific tertiary interactions. The structural and dynamic properties of cyt *c* bound to vesicles containing an anionic phospholipid (DOPS) were investigated by amide H-<sup>2</sup>H exchange using two-dimensional NMR spectroscopy and electrospray ionisation mass spectrometry. The H-<sup>2</sup>H exchange kinetics of the core amide protons in cyt *c*, which in the native protein undergo exchange *via* an uncorrelated EX2 mechanism, exchange in the lipid vesicles *via* a highly concerted global transition that exposes these protected amide groups to solvent. The lack of pH dependence and the observation of distinct populations of deuterated and protonated species by mass spectrometry confirms that exchange occurs *via* an EX1 mechanism with a common rate of  $1(\pm 0.5) \text{ h}^{-1}$ , which reflects the rate of transition from the lipid-inserted state, H', to an unprotected conformation, D', associated with the lipid interface.

© 2000 Academic Press

**Keywords:** cytochrome *c*; ESI MS; H-<sup>2</sup>H exchange kinetics; lipid-protein interactions; protein unfolding

\*Corresponding author

## Introduction

The interaction of water-soluble proteins with membranes is a common event occurring during the course of various cellular processes. Examples include the action of bacterial toxins in host cell membranes (Parker & Pattus, 1993) and the transfer of various non-polar ligands, such as retinol and fatty acids, to a target cell surface (Godovac-Zimmermann, 1988; Sacchetti *et al.*, 1988). The molecular mechanism by which soluble proteins bind and insert into biological membranes is not clearly understood. In the few cases studied, it appears that a partial unfolding of the water-soluble native structure of the protein leads to the exposure of hydrophobic patches onto the protein

surface, which triggers the insertion of the protein into the membrane (Merrill *et al.*, 1990; van der Goot *et al.*, 1991). The mechanism is complex and appears to involve both electrostatic and hydrophobic lipid-protein interactions (Heymann *et al.*, 1996).

Cytochrome *c* (Cyt *c*) has been widely used as a model protein for elucidating the interaction of water-soluble proteins with membranes (Rietveld *et al.*, 1983; Mustonen *et al.*, 1987; Pinheiro & Watts, 1994a,b; Pinheiro, 1994). This small protein (~ 12 kDa) functions in electron transfer on the surface of the inner mitochondrial membrane. It has been a matter of controversy whether a membrane-bound form of cyt *c* would be involved in electron transfer (Vik *et al.*, 1981; Speck *et al.*, 1983; Gupte & Hackenbrock, 1988; Hildebrandt *et al.*, 1990). However, more recently it has been shown that under physiological conditions cyt *c* is found to exist in an equilibrium between the soluble state and conformations bound to the inner mitochondrial membrane (Cortese *et al.*, 1998). These membrane-bound species have a destabilised structure

Abbreviations used: cyt *c*, horse heart cytochrome *c*; ESI MS, electrospray ionisation mass spectrometry; DOPS, dioleoylphosphatidylserine (1,2-dioleoyl-*sn*-glycero-3-phosphoserine); H-<sup>2</sup>H, hydrogen-deuterium; NOE, nuclear Overhauser enhancement.

E-mail address of the corresponding author: [tpinheiro@bio.warwick.ac.uk](mailto:tpinheiro@bio.warwick.ac.uk)

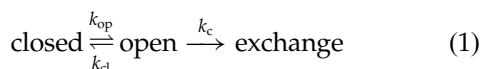
compared with the native protein, but retain variable degrees of electron transfer activities, depending on their binding state to the inner mitochondrial membrane. This suggests that membrane-bound forms of cyt *c* could regulate the activity of electron transfer *in vivo*.

Despite cyt *c* being one of the most studied proteins during the past half-century, the recent years have uncovered an unexpected role of cyt *c* in cell signalling, when Liu *et al.* (1996) found that programmed cell death (apoptosis) requires the release of cyt *c* from the mitochondrion. The surprises have not stopped there. A recent report by Jemmerson *et al.* (1999) has shown that a membrane-bound form of cyt *c* has apoptotic activity, suggesting that membrane-associated cyt *c* might be the relevant factor in caspase activation. It is known that the binding of cyt *c* to negatively charged lipid membranes induces an extensive disruption of the native compact structure of the protein (Muga *et al.*, 1991; de Jongh *et al.*, 1992; Spooner & Watts, 1991; Pinheiro & Watts, 1994a; Pinheiro *et al.*, 1997). This membrane-bound state lacks many features of its native tertiary structure but remains highly helical, with an overall content of  $\alpha$ -helical structure similar to that of the native protein in solution. Tryptophan fluorescence and haem absorbance kinetics have shown that the disruption of the tightly packed native structure of cyt *c* is dramatically accelerated on the membrane interface relative to the unfolding rate of the free protein in solution (Pinheiro *et al.*, 1997).

The growing evidence for physiological roles of membrane-bound forms of cyt *c*, both in electron transfer (Cortese *et al.*, 1998) and in apoptosis (Jemmerson *et al.*, 1999), makes studying the interaction of cyt *c* with lipid membranes of particular importance. It is apparent that structural and dynamic information on membrane-associated forms of cyt *c* will bring further insight into the mechanisms by which this protein carries out such diverse cellular functions. Here, we have characterised the structural and dynamic behaviour of membrane-bound cyt *c* using H-<sup>2</sup>H exchange kinetics in combination with NMR spectroscopy and electrospray ionisation (ESI) mass spectrometry (MS). It was found that the reversible binding of cyt *c* to the membrane is a highly cooperative transition, which leads to the disruption of all native tertiary contacts typical of the tight fold of native cyt *c*.

### EX1 and EX2 limits

According to the Linderström-Lang model (Linderström-Lang, 1955), the H-<sup>2</sup>H exchange reaction of a protected amide only takes place after its proton becomes exposed to solvent as a result of structural opening, as illustrated in equation (1):



where  $k_{\text{op}}$  and  $k_{\text{cl}}$  are the rate constants for the opening and closing processes, respectively, and  $k_{\text{c}}$  is the intrinsic rate of chemical exchange of the amide exposed to solvent. Intrinsic amide exchange rates depend on pH and local sequence and have been calculated for short unstructured peptides (Bai *et al.*, 1993). Under native conditions ( $k_{\text{cl}} \gg k_{\text{op}}$ ), the rate constant for the overall exchange reaction ( $k_{\text{ex}}$ ) is given by:

$$k_{\text{ex}} = \frac{k_{\text{op}}k_{\text{c}}}{k_{\text{op}} + k_{\text{cl}} + k_{\text{c}}} \quad (2)$$

equation (2) is often simplified by considering two limits for exchange (Hvidt & Nielsen, 1966). In the common EX2 limit, where  $k_{\text{cl}} \gg k_{\text{c}}$ , chemical exchange is the rate-limiting step, and equation (2) reduces to:

$$k_{\text{ex}} = \frac{k_{\text{op}}}{k_{\text{cl}}}k_{\text{c}} = K_{\text{op}}k_{\text{c}} \quad (3)$$

where  $K_{\text{op}}$  is the equilibrium constant for the conformational transition between the closed and open states. The other exchange limit, known as the EX1 limit, occurs when  $k_{\text{cl}} \ll k_{\text{c}}$ , and equation (2) is simplified to:

$$k_{\text{ex}} = k_{\text{op}} \quad (4)$$

Under EX2 conditions many openings occur for each successful amide-exchange event, and the exchange kinetics can be used to study the equilibrium between closed and open states, while in the EX1 limit each opening leads to exchange and the observed exchange rate is a measure of the opening rate. Also, because exchange is catalysed by acid and base,  $k_{\text{c}}$  is dependent on pH (Eigen, 1964). Therefore, in the EX2 limit the observed exchange rates ( $k_{\text{ex}}$ ) are strongly pH dependent (equation (3)), whereas under EX1 conditions (equation (4)) the observed exchange rate is independent of pH (Roder *et al.*, 1985). Furthermore, EX2 exchange is always random or uncorrelated for different amide sites in the protein, regardless of whether cooperative unfolding occurs. In contrast, under EX1 conditions, exchange among different amides can be correlated as shown by nuclear Overhauser enhancement (NOE) measurements of partly exchanged samples (Roder *et al.*, 1985) or ESI MS (Miranker *et al.*, 1993), provided that the underlying conformational event, i.e. structural opening or local unfolding, is cooperative.

### Results

To measure the kinetics of hydrogen exchange for cyt *c* bound to DOPS vesicles, we used both NMR spectroscopy and ESI mass spectrometry in conjunction with a quenched hydrogen exchange protocol (see Materials and Methods). The main advantage of this approach is that, while H-<sup>2</sup>H exchange occurs in the presence of lipid vesicles,

NMR and/or ESI MS analysis can be performed under native conditions, after precipitating the lipid and refolding cyt *c* under slow-exchange conditions. While H-<sup>2</sup>H exchange combined with NMR provides the rates of amide exchange of individual amides in the protein, measurements by ESI MS report on the overall amide-exchange properties and distribution of states.

### Resolved amide exchange rates by NMR

Representative exchange curves for distinct amides involved in different structural sites in cyt *c* are shown in Figure 1(a)-(c). Lys13 is located in the N-terminal  $\alpha$ -helix, Leu32 is part of a type II  $\beta$ -turn, Met65 and Tyr74 are in the middle of the 60s and 70s helices, respectively, while Leu98 and Lys100 are part of the C-terminal  $\alpha$ -helix (Bushnell *et al.*, 1990). The 40 amide sites that can be resolved by NMR show very similar H-<sup>2</sup>H exchange rates of  $0.95(\pm 0.52) \text{ h}^{-1}$  at pH 7.0, and  $0.98(\pm 0.62) \text{ h}^{-1}$  at pH 8.0 (errors are the standard deviations of 40 amides), which are remarkably consistent with the overall amide-exchange rate measured by ESI MS (Figure 1(d); see below). The wide range of exchange rates for native cyt *c* in solution is converted to a narrow range of rates for both pH values (Figure 2), which overlaps with the fastest measured rates within this group of amides for the exchange in solution. The narrow range of exchange rates observed for the 40 core amides in cyt *c* bound to DOPS vesicles, in addition to their similar values for the two pH values analysed

here, strongly suggest an exchange regime in the EX1 limit.

Under EX1 conditions (equation (4)) there need be no pH dependence of the observed exchange rate ( $k_{\text{ex}}$ ), whereas in the EX2 limit (equation (3))  $k_{\text{ex}}$  will be dependent on the concentration of H<sub>3</sub>O<sup>+</sup> or OH<sup>-</sup> in the acid or base-catalysed exchange reaction. Therefore, in the base-catalysed region, a significant positive slope ( $\sim 1$  if  $K_{\text{op}}$  is pH independent) for a plot of  $\log k_{\text{ex}}$  against pH indicates EX2 exchange limit. On the other hand, the slope would be smaller or zero under EX1 conditions, where the pH-dependent  $k_c$  no longer contributes to exchange. Figure 3(a) shows that the exchange rates measured under native solution conditions are at least an order of magnitude higher at pH 8 compared to pH 7, which is fully consistent with an EX2 mechanism (Jeng *et al.*, 1990; Milne *et al.*, 1998). The exchange rates for many amide protons (especially the more slowly exchanging ones which experience relatively global structural transitions) are significantly higher than those expected for an EX2 mechanism with pH-independent  $K_{\text{op}}$  (broken line), indicating that the pH-dependent destabilisation of the protein tends to shift the conformational equilibrium toward more open states. In contrast, the corresponding plot for the exchange rates of cyt *c* bound to DOPS vesicles shows a much tighter distribution of largely pH-independent rates (Figure 3(b)). However, the 32 amide protons for which rates could be measured at both pH values tend to fall into three distinct groups. A group of 14 amides (group I) appears to undergo exchange under a pH independent EX1 mechanism associ-

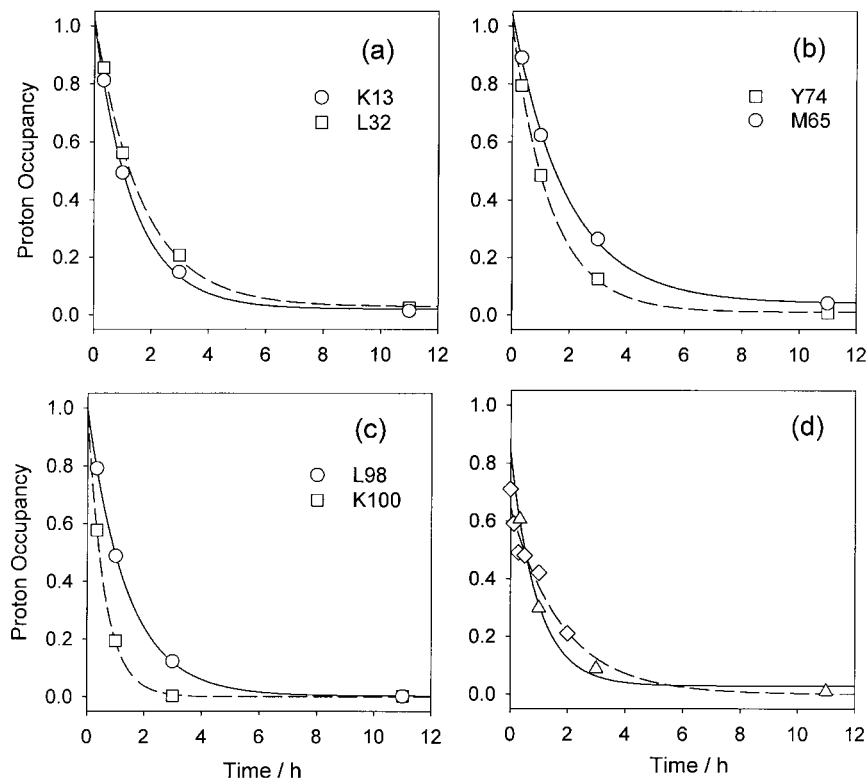


**Figure 1.** Kinetics of the H-<sup>2</sup>H exchange of cyt *c* in DOPS membranes at 20°C (pH 7.0). The proton occupancy of representative backbone amide sites of cyt *c* measured by NMR (from a total of 40 amides) is plotted as a function of exchange times ((a)-(c)). (d) shows the global (28 participating protons, see the text) amide exchange at pH 7 (triangles) or pH 8 (diamonds) measured by ESI MS. The curves represent exponential fits to the experimental data points determined by non-linear least-squares analysis. Proton occupancy was calculated from normalised NOE intensities of COSY NMR spectra or peak intensities of mass spectra (see Materials and Methods). Estimated errors in the rate constants (see Figure 2) are in the range 10-30%.

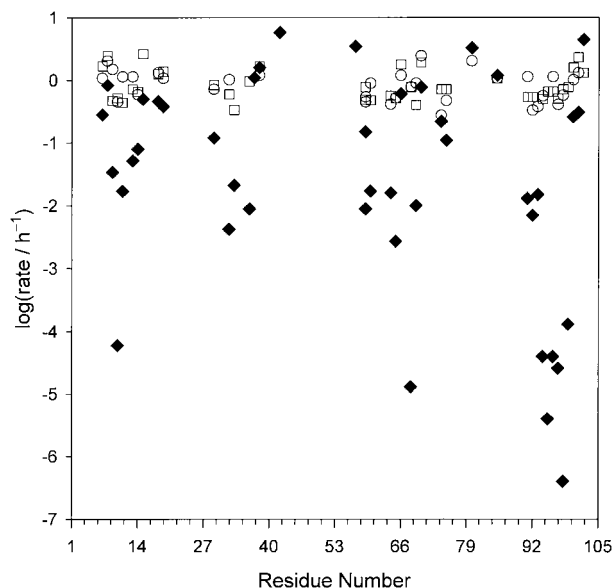


**Figure 2.** The H<sup>2</sup>H exchange rates at 20 °C of various amide protons resolved by NMR for *cyt c* bound to DOPS vesicles at pH 7.0 (circles) and 8.0 (squares) in comparison with the exchange of native *cyt c* in solution at pH 7.0 (diamonds). Estimated error bars (standard fitting errors) are comparable to or smaller than the symbols.

ated with an average  $k_{op}$  of  $0.6(\pm 0.2) \text{ h}^{-1}$ . A second group of ten amides (group II) is also consistent with a pH-independent EX1 mechanism but associated with a faster opening rate of  $1.6(\pm 0.5) \text{ h}^{-1}$ . The third group of eight amides (group III) show an EX1 mechanism with a negative pH dependence and associated with a  $k_{op}$  of  $1.1(\pm 0.2) \text{ h}^{-1}$  at pH 7 and  $0.5(\pm 0.1) \text{ h}^{-1}$  at pH 8. An examination of the distribution of these amides within the native structure of *cyt c* revealed that group I is composed of amides predominantly associated with apolar residues buried within the hydrophobic core, whereas groups II and III are mainly associated with polar residues located in loop regions or the ends of helices.

### Global amide exchange by ESI MS

Once it was shown that mass differences associated with deuterium incorporation were measurable by mass spectrometry (Katta & Chait, 1991), MS has become a valuable tool for H<sup>2</sup>H exchange studies of protein folding (Miranker *et al.*, 1993; Yi & Baker, 1996; Arrington *et al.*, 1999). Unlike the NMR approach, MS cannot provide individual amide-exchange rates, but has the advantage of probing directly the nature of cooperative transitions, providing a straightforward method for distinguishing between EX1 and EX2 mechanisms, as well as the continuum of possibilities in between (Miranker *et al.*, 1996). If the exchange occurs in the EX1 limit (equation (4)) each opening reaction (equation (1)) leads to the exchange of all labile

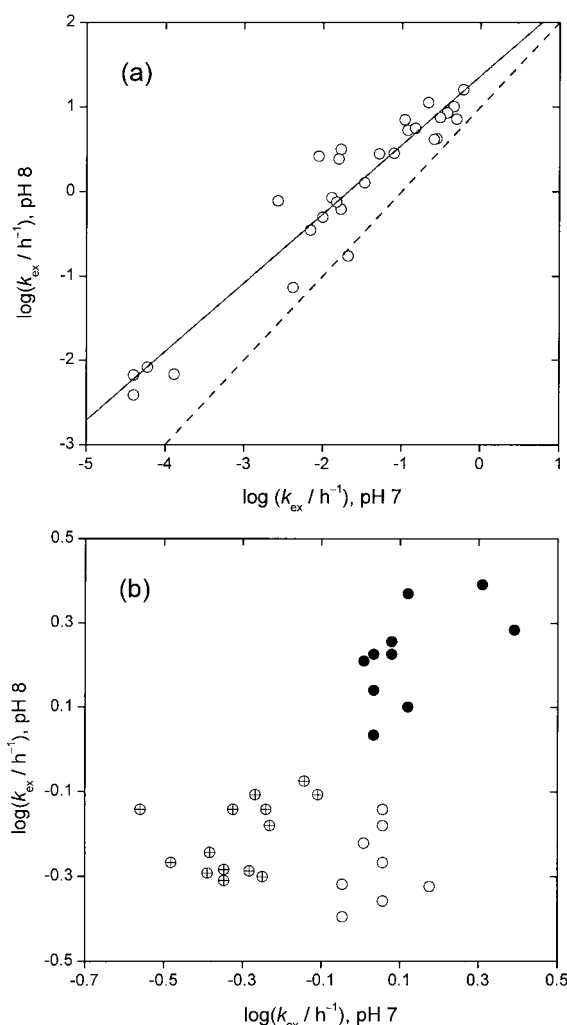


**Figure 3.** Plots of amide hydrogen exchange rates at 20 °C measured at two values of pH. The value of  $\log k_{ex}$  for each residue at pH 7 is plotted against their corresponding values at pH 8 for the exchange of free *cyt c* in solution (a) and when bound to DOPS vesicles (b). In (a), the continuous line represents a linear regression fit to the experimental data points, and the broken line indicates the expected rates under EX2 conditions with  $K_{op}$  independent of pH. (b) illustrates the much narrower range of rates and limited pH dependence observed in the presence of lipid vesicles. Three groups of amide protons are highlighted: group I (crossed circles), with the slow pH-independent exchange rate of  $0.6(\pm 0.2) \text{ h}^{-1}$ ; group II (filled circles), with the faster exchange rate of  $1.6(\pm 0.5) \text{ h}^{-1}$  also independent of pH; and group III (open circles), with an average rate at pH 7 of  $1.1(\pm 0.2) \text{ h}^{-1}$  decreasing to  $0.5(\pm 0.1) \text{ h}^{-1}$  at pH 8.

sites exposed in the transition. This results in a mass spectrum with two distinct peaks whose masses reflect the fully protonated and fully deuterated species and whose intensities indicate the overall extent of exchange. In contrast, under EX2 conditions (equation (3)) H<sup>2</sup>H exchange will occur at random positions in individual protein molecules as a result of relatively frequent but short

visits to the open state. In this regime the resulting mass spectrum will contain one single peak whose position shifts with exchange time. The same spectral pattern will also exist under EX1 conditions when molecular fluctuations are uncorrelated or non-cooperative.

Figure 4(a) shows the ESI mass spectrum of protonated cyt *c* in solution in comparison with the spectra of fully and partially deuterated forms of cyt *c* in solution. The protonated and fully deuterated forms show a mass difference of 202, which corresponds to the total number of labile protons in the protein. The partially deuterated state, illustrated by the peak at 12,518 Da, is that of a freshly transferred protein sample into  $^2\text{H}_2\text{O}$  (pH 5). This state has all fast ( $k_{\text{ex}} > 10 \text{ h}^{-1}$ ) amide protons exchanged for deuterons and a core of 42 amides which are more resistant to exchange. This core of protected amides represents the group of measurable amides by NMR. Figure 4(b) compares the mass spectra of this control sample with those recorded on aliquots of the cyt *c* samples

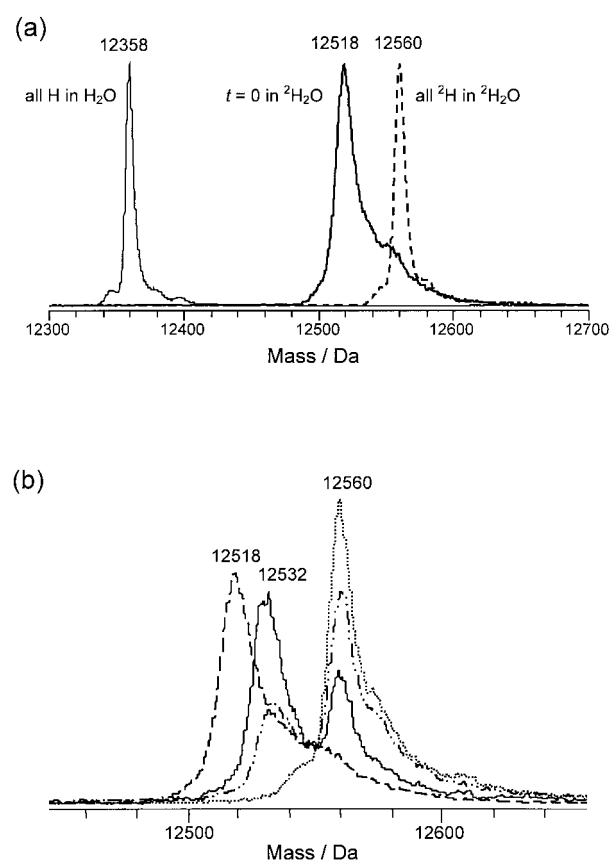


**Figure 4.** ESI mass spectra of cyt *c* (a) in  $\text{H}_2\text{O}$  buffer solution (all H in  $\text{H}_2\text{O}$ ); freshly transferred into  $^2\text{H}_2\text{O}$  buffer ( $t = 0$  in  $^2\text{H}_2\text{O}$ ); and fully exchanged in  $^2\text{H}_2\text{O}$  buffer solution (all  $^2\text{H}$  in  $^2\text{H}_2\text{O}$ ); and (b) in the presence of DOPS vesicles at various exchange times: 20 minutes (continuous line); one hour (broken-dotted line) and 11 hours (dotted line), in comparison with freshly transferred cyt *c* into  $^2\text{H}_2\text{O}$  buffer ( $t = 0$  in  $^2\text{H}_2\text{O}$ ; broken line).

exchanged in the presence of DOPS, following NMR analysis. During the exchange of cyt *c* bound to DOPS vesicles the peak at 12,518 Da first shifts to 12,532 Da for the first measured exchange time (seven minutes, data not shown). This 14 Da shift reflects the loss of protons during the time needed to separate the refolded cyt *c* from lipids and to prepare NMR samples ( $\sim$ two hours in  $^2\text{H}_2\text{O}$  at pH 5.3 and  $4^\circ\text{C}$ ), and during 2D NMR data acquisition ( $\sim$ four hours at  $20^\circ\text{C}$ ). Under these conditions exchange is expected to occur *via* an uncorrelated EX2 mechanism. This was confirmed by recording a series of ESI MS spectra on a test sample (20  $\mu\text{M}$  cyt *c* in  $^2\text{H}_2\text{O}$ , 10 mM ammonium acetate (pH 5.0),  $25^\circ\text{C}$ ), which showed a single peak that slowly moved with time toward higher mass. The exchange rates for the  $\sim$ 30 amides protons remaining under native conditions after NMR analysis are sufficiently slow so that no additional exchange occurs during ESI MS analysis. For all quenched  $\text{H}^2\text{H}$  exchange samples monitored by ESI MS, two peaks were observed in the mass spectra at 12,532 and 12,560 Da, corresponding to partially and fully exchanged forms of the protein, respectively (Figure 4(b)). During the course of exchange the peak at 12,532 Da decreased in intensity as the peak of fully deuterated species at 12,560 Da increased. The mass difference between these two peaks corresponds to 28 protons, which, as the ESI mass spectra indicate, undergo  $\text{H}^2\text{H}$  exchange under an EX1 mechanism. The overall exchange rate for this group of amides was calculated from the exponential fit in Figure 1(d) and found to be  $1.1(\pm 0.2) \text{ h}^{-1}$  (see Materials and Methods). This rate is well within error of the average exchange rate measured by NMR analysis of the same series of cyt *c* samples, which confirms that ESI MS, in conjunction with quenched  $\text{H}^2\text{H}$  exchange procedures, provides a reliable measure of  $\text{H}^2\text{H}$  exchange in proteins. Also shown in Figure 1(d) are the results of ESI MS measurements on a series of quenched samples exchanged in DOPS vesicles at pH 8. These samples were prepared specially for MS analysis under conditions matching the NMR experiment at pH 8, but at  $\sim$ fivefold lower protein concentration (see Materials and Methods). As in the study at pH 7 (Figure 4(b)), the mass spectra showed two peaks separated by 28 mass units corresponding to a group of core protons that exchange *via* a concerted (EX1) exchange mechanism. The exponential decay of the relative population of the protonated species with exchange time yields a rate constant of  $0.6(\pm 0.1) \text{ h}^{-1}$ , which is again in good agreement with the NMR results, matching the exchange rate of protons in groups I and III (Figure 3(b)). The slight decrease in the rate on raising the pH from 7 to 8 is in marked contrast with the more than tenfold increase in exchange rate measured under native conditions, which further supports our conclusion that exchange in the presence of DOPS is governed by an unusual EX1 mechanism.

## Discussion

The amide-exchange rates determined by NMR of the core residues of *cyt c* when bound to DOPS vesicles show a remarkably narrow spread in comparison with the exchange behaviour of native *cyt c* in solution (Figure 2). The range of rates observed (less than a factor of 10) is narrower than that expected for the corresponding intrinsic rates (Bai *et al.*, 1993) and there is no apparent correlation between  $k_{\text{ex}}$  and  $k_c$ . This observation, combined with the pH independence between pH 7 and 8 for most of the exchange rates, provides strong evidence for an EX1 mechanism, associated with a highly concerted global conformational transition of *cyt c* that exposes all the amides to solvent. A closer inspection of the dependence of  $k_{\text{ex}}$ , as shown in Figure 3(b), revealed a tendency for protons to cluster into three groups: one with a slow exchange rate around  $0.6 \text{ h}^{-1}$  (group I), a faster group with an exchange rate around  $1.6 \text{ h}^{-1}$  (group II), both of which are independent of pH, and a subset of protons switching from a faster rate  $\sim 1.1 \text{ h}^{-1}$  at pH 7 to a slower rate  $\sim 0.5 \text{ h}^{-1}$  at pH 8 (group III).

Our analysis of H-<sup>2</sup>H exchange in lipid-bound *cyt c* using ESI MS revealed two separate peaks in the mass spectra of partially exchanged samples (Figure 4(b)), which indicates that a large group of

amides (28 of the 42 core amides) exchange *via* a highly concerted global unfolding transition that exposes all these otherwise protected protons to solvent. The partially protonated species corresponding to the peak at 12,532 Da undergo cooperative EX1 exchange of all their amide protons, resulting in the fully deuterated species with a mass of 12,560 Da. Therefore, the overall H-<sup>2</sup>H exchange of the core amides of *cyt c* in DOPS membranes occurs *via* an EX1 mechanism, with most amides ( $\sim 67\%$ , corresponding to 28 out of 42 core amides) associated with a highly cooperative conformational transition of *cyt c*.

The combined exchange results, monitored both by NMR spectroscopy and ESI mass spectrometry, led us to propose a kinetic mechanism for the interaction of *cyt c* with negatively charged lipid membranes of DOPS, illustrated in Figure 5. In this scheme  $N^w$  represents the native state of *cyt c* in aqueous solution,  $N^*$  denotes a native-like state associated with the membrane surface,  $D^i$  depicts an open conformation of the protein associated with the membrane interface, and  $H^l$  is the final lipid-inserted helical state. The binding of *cyt c* to the membrane surface ( $N^w \rightarrow N^*$ ) is driven by the electrostatic attraction between polar residues on the protein surface and the negative lipid head-groups in the membrane. Since diffusion-controlled association is likely to be accelerated by favourable

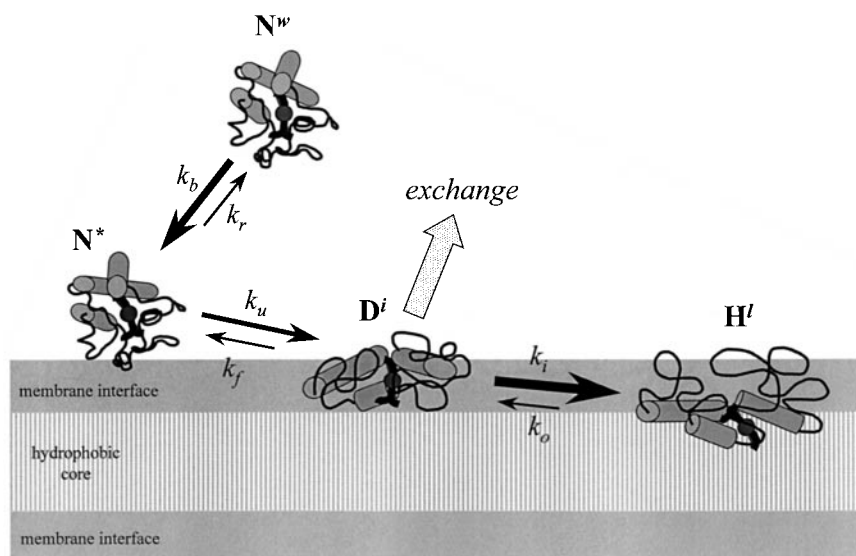


**Figure 5.** Proposed kinetic mechanism for the interaction of *cyt c* with negatively charged lipid membranes of DOPS.  $N^w$  represents the folded native conformation of *cyt c* in aqueous solution,  $N^*$  a native-like state bound to the membrane surface,  $D^i$  denotes a denatured state associated with the membrane interface, and  $H^l$  is the final lipid-inserted helical state. The reactions are labelled with their suggestive rate constants:  $k_b$  for the binding step  $N^w \rightarrow N^*$ ;  $k_r$  for the release of *cyt c* from the membrane surface,  $N^* \rightarrow N^w$ ;  $k_u$  for the unfolding reaction  $N^* \rightarrow D^i$ ;  $k_f$  for the reverse folding reaction  $D^i \rightarrow N^*$ ;  $k_i$  denotes the insertion step of the open state on the membrane interface ( $D^i$ ) into the hydrophobic core of the lipid membrane ( $D^i \rightarrow H^l$ );  $k_o$  is the rate of the back reaction associated with the transition from the lipid-protected state to the open, unprotected state in the membrane interface ( $H^l \rightarrow D^i$ ). A majority of amide protons observed are protected in  $H^l$ , but exchange rapidly in the surface-associated state  $D^i$ , giving rise to correlated EX1 exchange behaviour. Protein and membrane are drawn in relative proportional dimensions: diameter native *cyt c*,  $\sim 30 \text{ \AA}$ ; interface thickness,  $\sim 15 \text{ \AA}$ ; and hydrophobic core of the lipid bilayer,  $\sim 30 \text{ \AA}$ .

electrostatic interactions, binding is expected to be very fast ( $k_b \gg 1000 \text{ s}^{-1}$ ) and release ( $k_r$ ) of the protein from the membrane surface to be unfavourable ( $k_r \ll k_b$ ). The environment of the membrane interface triggers the subsequent partial unfolding of cyt *c* ( $N^* \rightarrow D^i$ ). Lipid-induced unfolding is thought to be facilitated by the local acidic environment of the membrane surface (Bychkova & Ptitsyn, 1993; Pinheiro *et al.*, 1997). In addition, the new electrostatic bonding between charged residues in the protein and lipid headgroups at the membrane surface, which is generally an exothermic process, could provide the energy necessary for the main protein unfolding step. We have shown that the compact native-like structure associated with the membrane surface ( $N^*$ ) is converted to the denatured state  $D^i$  associated with the membrane interface at a rate  $k_u \sim 1.5 \text{ s}^{-1}$  (Pinheiro *et al.*, 1997). This partially unfolded intermediate is then able to insert, at least partially, into the hydrophobic core of the lipid membrane ( $H^l$ ). Once  $D^i$  is formed, insertion is expected to be very fast ( $k_i \gg k_u$ ) leading to the protected state  $H^l$ . Exchange is then limited by the rate of conversion of the lipid-buried  $H^l$  state into the interface-associated unprotected state  $D^i$ . Therefore, the correlated EX1 rate of exchange,  $k_{\text{ex}} \sim 1 \text{ h}^{-1}$ , reflects the opening rate ( $k_o$ ) associated with the step  $H^l \rightarrow D^i$ . According to the nomenclature in equation (1),  $H^l$  corresponds to the closed state,  $D^i$  to the open state, and  $k_o$  to  $k_{\text{op}}$ .

Based on equilibrium spectroscopic data (Pinheiro *et al.*, 1997), the lipid-inserted state  $H^l$  has been shown to retain a native-like  $\alpha$ -helical structure, but has a highly perturbed tertiary conformation in terms of (a) enhanced Trp59 fluorescence, which indicates that the average distance between Trp59 and the haem is much larger than in the native state, (b) lack of specific tertiary interactions involving Trp59, as revealed by near-UV CD and (c) a disturbed haem ligation and haem environment, as shown by Soret absorbance and CD. The protected state  $H^l$  is likely to contribute to exchange *via* amides associated with polar residues in loop regions of the protein, which are expected to reside in the interface of the lipid membrane. This lipid-protected state need not be a compact conformation, as protection against  $\text{H-}^2\text{H}$  exchange would result from the stabilisation of  $\alpha$ -helical H-bonds due to insertion into the hydrophobic core of the lipid membrane (Figure 5). This state is unlikely to involve inserted helices in a transmembrane orientation. Instead, as the Figure suggests, the amphipathic  $\alpha$ -helices of cyt *c* are more likely to lie flat on the membrane interface with the hydrophobic face towards the hydrocarbon core of the lipid bilayer. The apolar portion of the haem group is expected to insert into the hydrophobic domain of the membrane (Cannon *et al.*, 1984), and the absence of a blue shift of the Soret absorbance band (Pinheiro *et al.*, 1997) suggests that the haem iron atom retains an octahedral coordination, prob-

ably involving non-native axial ligands from the protein or lipid headgroup.

In conclusion, the overall EX1 exchange mechanism observed for the core amide protons of cyt *c* requires a highly concerted global conformational event that would expose these, otherwise protected, amides to the aqueous environment of the lipid interface. Therefore, the unprotected denatured state  $D^i$  is likely to be a very open state, at least at the level of the tertiary structure. However, we expect that this state may be as helical as  $H^l$ . This interpretation is supported by the fact that formation of secondary structure alone is insufficient to account for the high protection to  $\text{H-}^2\text{H}$  exchange seen in the core of native proteins, and that tertiary interactions are essential to stabilise the structure (Guijarro *et al.*, 1995; Finucane & Jardetzky, 1996). In fact, stopped-flow CD measurements of cyt *c* refolding in solution showed a 44% regain of secondary structure after 4 ms, while pulsed  $\text{H-}^2\text{H}$  exchange showed only 10-15% protection after 3 ms (Elöve *et al.*, 1992). Therefore, the partially helical, but open, conformation associated with the membrane interface ( $D^i$ ) appears to be the state responsible for EX1 exchange (Figure 5), while many protons are protected in  $H^l$  where much of the protein is buried within the hydrophobic region of the lipid membrane.

## Materials and Methods

### Reagents

Cyt *c* from horse heart (type IV) was purchased from the Sigma Chemical Co. and used without further purification. DOPS was purchased from Avanti Polar Lipids, Inc. (Birmingham, AL). Deuterium oxide ( $^2\text{H}_2\text{O}$ ,  $^2\text{H}$ , 99.9%),  $^2\text{HCl}$  ( $^2\text{H}$ , 99.5%),  $\text{NaO}^2\text{H}$  ( $^2\text{H}$ , 99.5%),  $^2\text{H}_3\text{PO}_4$  ( $^2\text{H}$ , 99.5%) and  $\text{C}^2\text{H}_3\text{CO}_2\text{H}$  ( $^2\text{H}$ , 99.9%) were obtained from Cambridge Isotope Laboratories.

### H- $^2\text{H}$ exchange

Aqueous protein solutions and lipid vesicles were prepared in 10 mM phosphate buffer (pH 7.0) or 10 mM Tris (pH 8.0). Protein concentrations were measured spectrophotometrically using a molar absorption coefficient of  $2.95 \times 10^4 \text{ M}^{-1} \text{ cm}^{-1}$  at 550 nm and pH 7.0 for the protein reduced with sodium dithionite (Margoliash & Walasek, 1967). Lipid vesicles were formed by the hydration of lyophilized DOPS with the required buffer, which was previously deoxygenated with argon gas, and all the steps of lipid hydration were carried out in an argon atmosphere. The resulting suspension of multilamellar lipid vesicles was sonicated for several periods of half an hour in a bath sonicator (Solidstate Ultrasonic FS-14, Fisher Scientific Brand), until a clear suspension of small unilamellar vesicles was obtained (on average for about three hours). This procedure has been shown to produce vesicles with diameters ranging from 300 to 600 Å in the absence of protein, and after protein binding these vesicles have diameters between 380 and 700 Å (Pinheiro *et al.*, 1997). The lipid-protein complex was preincubated in  $\text{H}_2\text{O}$  buffer for one hour at  $20^\circ\text{C}$  prior to  $\text{H-}^2\text{H}$  exchange, which was initiated by transferring the

sample into  $^2\text{H}_2\text{O}$  buffer, using Sephadex spinning columns at  $4^\circ\text{C}$ . The exchange was carried out at  $20^\circ\text{C}$ , at pH 7.0 or pH 8.0, and protein and lipid concentrations were  $100\ \mu\text{M}$  and  $10\ \text{mM}$ , respectively. Quenching of the exchange reaction was achieved by a twofold dilution of the exchange solution with  $4\ \text{M}\ \text{MgCl}_2$  in  $^2\text{H}_2\text{O}$ , containing  $50\ \text{mM}$  potassium phosphate,  $20\ \text{mM}$  potassium acetate, and  $6\ \text{mM}$  ascorbic acid (pH 5); simultaneously the temperature was dropped to  $4^\circ\text{C}$  by adding ice-chilled quenching buffer and transferring the exchange solution to ice. Upon addition of the quench solution the lipid vesicles were disrupted and cyt *c* dissociated into the aqueous solution. Under these conditions, the time scale of exchange for all amide protons, including those not yet involved in folded structure, is slow (1-30 minutes; Roder *et al.*, 1988) compared to the time of refolding for the lipid-dissociated protein ( $<100\ \text{ms}$ ; Elöve *et al.*, 1992) so that amide protons are effectively trapped in the refolded state. Excess ascorbic acid ( $6\ \text{mM}$ ) was included in the quench solution, reducing cyt *c* to its more stable ferrous haem state in which the exchange rate for most amide protons is slower (Wand *et al.*, 1986). Approximately 70% of the protein is recovered from the lipid complexes. After spinning at  $2000\ \text{g}$  on a benchtop Sorvall RT 6000D centrifuge, for half an hour at  $4^\circ\text{C}$ , a lipid film is separated from the lipid-free cyt *c* solution. The protein is kept reduced with excess ( $6\ \text{mM}$ ) ascorbic acid, concentrated and exchanged into the NMR buffer ( $50\ \text{mM}\ ^2\text{H}_3\text{PO}_4$ ,  $20\ \text{mM}\ \text{C}^2\text{H}_3\text{CO}_2\text{H}$ ,  $6\ \text{mM}$  ascorbic acid (pH 5.3)) using Millipore ultrafree-15 centrifugal filter devices with a molecular mass cut-off of  $5000\ \text{Da}$ . For  $^2\text{H}_2\text{O}$  solutions, pH measurements are direct readings from a standard glass electrode without adjustment for isotope effects Connelly *et al.*, 1993).

### NMR spectroscopy

NMR spectra were recorded at  $600.13\ \text{MHz}$  on a Bruker DMX 600 spectrometer. Two-dimensional (*J*-correlated COSY) spectra of reduced cyt *c* were acquired at  $20^\circ\text{C}$  at pH 5.3 on  $350\ \mu\text{l}$  samples of  $1\text{--}2\ \text{mM}$  protein. Typically 16-32 scans of 2048 complex data points were collected for 512 increments, with a recycle delay time of 1.6 seconds. NMR data were processed and analysed using FELIX97 (Molecular Simulations, Inc.). Cosine apodisation was applied prior to Fourier transformation in both dimensions. The final size of the transformed spectra was  $1024 \times 1024$  data points. Weak water suppression was used in order to minimise the loss of amide peak intensities near the water resonance.

### ESI mass spectrometry

For ESI MS analysis, a small aliquot was removed from each NMR sample, following exchange in lipid vesicles at pH 7 and NMR analysis. The refolded cyt *c* samples (in the absence of lipid) were diluted to  $\sim 10\ \mu\text{M}$  and transferred into  $1\ \text{mM}$  ammonium acetate in  $^2\text{H}_2\text{O}$  under native slow-exchange conditions (pH 5), using rapid Sephadex G25 gel filtration (spin columns with  $3\ \text{ml}$  bed volume and  $0.5\ \text{ml}$  sample volume). To facilitate electrospray ionisation, 5% (v/v) methanol (99 atom-%  $^2\text{H}$ ) was added immediately before infusion.

For the exchange measurements in DOPS vesicles at pH 8, a second series of cyt *c* samples was prepared specially for the MS analysis, using a quenched-exchange protocol similar to that described above, except for the initial concentration of cyt *c* ( $25\ \mu\text{M}$ ) and the final buffer

conditions. Following lipid extraction, the refolded and ascorbate-reduced cyt *c* samples were transferred into  $10\ \text{mM}$  ammonium acetate  $^2\text{H}_2\text{O}$  buffer at pH 5, using Sephadex G25 spin columns. The samples were loaded into a quartz nanospray capillary and infused directly under native conditions, without the addition of methanol. Mass spectra in the presence and absence of 5% deuterated methanol were indistinguishable.

Mass spectra were recorded on an LCQ quadrupole ion-trap mass spectrometer (Finnigan) with the full MS target volume set at  $5 \times 10^7$  for automatic gain control. Electrospray was accomplished by direct infusion of the samples ( $1\ \mu\text{l}/\text{min}$ ) into the Finnigan microspray ion source, using the following parameters:  $4.5\ \text{kV}$  spray voltage,  $220^\circ\text{C}$  heated capillary temperature,  $\text{N}_2$  sheath gas pressure of 70 to  $100\ \text{psi}$ . Signals were averaged for three to ten minutes and the neutral mass spectra of cyt *c* were obtained by deconvoluting the multiple-charged envelopes using the BIOMASS deconvolution software supplied by Finnigan.

### H- $^2\text{H}$ exchange rates

NMR-resolved amide H- $^2\text{H}$  exchange rates were calculated from the integrated volume for resolved NH-C $^2\text{H}$  cross-peaks, internally normalised to the non-exchanging haem bridge  $4\ \text{CH}_3\text{CH}$ . Amide proton peak heights in one-dimensional spectra were also used for well-resolved amides after subjecting samples to a second exchange (30 minutes at pH 10), which leaves eight to ten of the most highly protected amides. The global amide-exchange rate measured by ESI MS was obtained from the normalised intensities of the peaks at  $12,532$  and  $12,560\ \text{Da}$ , and expressed as a fraction of proton occupancy. Amide-exchange rates were calculated from non-linear least-squares analysis, and both NMR and ESI data points were found to fit a single exponential curve.

### Acknowledgements

This work has been supported by the Royal Society, the Human Frontier Science Programme (T.J.T.P.), by NIH grants GM35926 and GM56250 (H.R.), and by NIH Grant CA06927 and an appropriation from the Commonwealth of Pennsylvania to the Institute for Cancer Research. The NMR and mass spectrometry facilities (Fox Chase) are supported by grants from the Kresge and Fannie E. Rippel Foundations, respectively. T.J.T.P. is a Royal Society University Research Fellow. We thank Gülnur A. Elöve for stimulating discussions in the early stages of this project, and Professor Keith Jennings for a critical reading of the manuscript.

### References

- Arrington, C. B., Teesch, L. M. & Robertson, A. D. (1999). Defining protein ensembles with native-state NH exchange: kinetics of interconversion and cooperative units from combined NMR and MS analysis. *J. Mol. Biol.* **285**, 1265-1275.
- Bai, Y., Milne, J. S., Mayne, L. & Englander, S. W. (1993). Primary structure effects on peptide group hydrogen exchange. *Proteins: Struct. Funct. Genet.* **17**, 4-14.

- Bushnell, G. W., Louie, G. V. & Brayer, G. D. (1990). High-resolution three-dimensional structure of horse cytochrome *c*. *J. Mol. Biol.* **214**, 585-595.
- Bychkova, V. E. & Ptitsyn, E. (1993). The molten globule *in vitro* and *in vivo*. *Chemtracts: Biochem. Mol. Biol.* **4**, 133-163.
- Cannon, J. B., Kuo, F.-S., Pasternack, R. F., Wong, N. M. & Muller-Eberhard, U. (1984). Kinetics of the interaction of heme liposomes with heme binding proteins. *Biochemistry*, **23**, 3715-3721.
- Connelly, G. P., Bai, Y., Jen, M.-F. & Englander, S. W. (1993). Isotope effects in peptide group hydrogen exchange. *Proteins: Struct. Funct. Genet.* **17**, 87-92.
- Cortese, J. D., Voglino, A. L. & Hackenbrock, C. R. (1998). Multiple conformations of physiological membrane-bound cytochrome *c*. *Biochemistry*, **37**, 6402-6409.
- de Jongh, H. H. J., Killian, J. A. & de Kruijff, B. (1992). A water lipid interface induces a highly dynamic folded state in apocytochrome *c* and cytochrome *c* which may represent a common folding intermediate. *Biochemistry*, **31**, 1636-1643.
- Eigen, M. (1964). Proton transfer, acid-base catalysis, and enzymatic hydrolysis. *Angew. Chem.* **3**, 1-19.
- Elöve, G. A., Chaffotte, A. F., Roder, H. & Goldberg, M. E. (1992). Early steps in cytochrome *c* folding probed by time-resolved circular dichroism and fluorescence spectroscopy. *Biochemistry*, **31**, 6876-6883.
- Finucane, M. D. & Jardetzky, O. (1996). The pH dependence of hydrogen-deuterium exchange in *trp* repressor: the exchange rate amide protons in proteins reflects tertiary interactions, not only secondary structure. *Protein Sci.* **5**, 653-662.
- Godovac-Zimmermann, J. (1988). The structural motif of  $\beta$ -lactoglobulin and retinol-binding protein: a basic framework for binding and transport of small hydrophobic molecules? *Trends Biochem. Sci.* **13**, 64-66.
- Guijarro, J. I., Jackson, M., Chaffotte, A. F., Delepierre, M., Mantsch, H. H. & Goldberg, M. E. (1995). Protein folding intermediates with rapidly exchangeable amide protons contain authentic hydrogen-bonded secondary structures. *Biochemistry*, **34**, 2998-3008.
- Gupte, S. S. & Hackenbrock, C. R. (1988). The role of cytochrome *c* diffusion in mitochondrial electron transport. *J. Biol. Chem.* **263**, 5248-5253.
- Heymann, J. B., Zakharov, S. D., Zhang, Y.-L. & Cramer, W. A. (1996). Characterization of electrostatic and nonelectrostatic components of protein-membrane binding interactions. *Biochemistry*, **35**, 2717-2725.
- Hildebrandt, P., Heimburg, T., Marsh, D. & Powell, G. L. (1990). Conformational changes in cytochrome *c* and cytochrome *c* oxidase upon complex formation: a resonance Raman study. *Biochemistry*, **29**, 1661-1668.
- Hvidt, A. & Nielsen, S. O. (1966). Hydrogen exchange in proteins. *Advan. Protein Chem.* **21**, 287-386.
- Jemmerson, R., Liu, J., Hausauer, D., Lam, K.-P., Mondino, A. & Nelson, R. D. (1999). A conformational change in cytochrome *c* of apoptotic and necrotic cells is detected by monoclonal antibody binding and mimicked by association of native antigen with synthetic vesicles. *Biochemistry*, **38**, 3599-3609.
- Jeng, M.-F., Englander, S. W., Elöve, G. A., Wand, A. J. & Roder, H. (1990). Structural description of acid-denatured cytochrome *c* by hydrogen exchange and 2D NMR. *Biochemistry*, **29**, 10433-10437.
- Katta, V. & Chait, B. T. (1991). Conformational changes in protein probed by hydrogen exchange and electrospray mass spectrometry. *Rapid Commun. Mass Spectrom.* **5**, 214-217.
- Linderström-Lang, K. U. (1995). Deuterium exchange between peptides and water. In *Symposium on Peptide Chemistry. Chem. Soc. Spec. Publ.* **2**, 1-20.
- Liu, X., Kim, C. N., Yang, J., Jemmerson, R. & Wang, X. (1996). Induction of apoptotic program in cell-free extracts: requirement for dATP and cytochrome *c*. *Cell*, **86**, 147-157.
- Margoliash, E. & Walasek, O. F. (1967). Cytochrome *c* from vertebrate and invertebrate sources. *Methods Enzymol.* **10**, 339-348.
- Merrill, A. R., Cohen, F. S. & Cramer, W. A. (1990). On the nature of the structural change of the colicin E1 channel peptide necessary for its translocation-competent state. *Biochemistry*, **29**, 5829-5836.
- Milne, J. S., Mayne, L., Roder, H., Wand, A. J. & Englander, S. W. (1998). Determinants of protein hydrogen exchange studied in equine cytochrome *c*. *Protein Sci.* **7**, 739-745.
- Miranker, A., Robinson, C. V., Radford, S. E., Aplin, R. T. & Dobson, C. M. (1993). Detection of transient protein folding populations by mass spectrometry. *Science*, **262**, 896-900.
- Miranker, A., Robinson, C. V., Radford, S. E. & Dobson, C. M. (1996). Investigation of protein folding by mass spectrometry. *FASEB J.* **10**, 93-101.
- Muga, A., Mantsch, H. H. & Surewicz, W. K. (1991). Membrane binding induces destabilization of cytochrome *c* structure. *Biochemistry*, **30**, 7219-7224.
- Mustonen, P., Virtanen, J. A., Somerharju, P. J. & Kinnunen, P. K. J. (1987). Binding of cytochrome *c* to liposomes as revealed by the quenching of fluorescence from pyrene-labeled phospholipids. *Biochemistry*, **26**, 2991-2997.
- Parker, M. W. & Pattus, F. (1993). Rendering a membrane protein soluble in water: a common packing motif in bacterial toxins. *Trends Biochem. Sci.* **18**, 391-395.
- Pinheiro, T. J. T. (1994). The interaction of horse heart cytochrome *c* with phospholipid bilayers. Structural and dynamic effects. *Biochimie*, **76**, 489-500.
- Pinheiro, T. J. T. & Watts, A. (1994a). Lipid specificity in the interaction of cytochrome *c* with anionic phospholipid membranes. *Biochemistry*, **33**, 2451-2458.
- Pinheiro, T. J. T. & Watts, A. (1994b). Resolution of individual lipids in mixed phospholipid membranes and specific lipid-cytochrome *c* interactions by magic-angle spinning solid-state phosphorus-31 NMR. *Biochemistry*, **33**, 2459-2467.
- Pinheiro, T. J. T., Elöve, G. A., Watts, A. & Roder, H. (1997). Structural and kinetic description of cytochrome *c* unfolding induced by the interaction with lipid vesicles. *Biochemistry*, **36**, 13122-13132.
- Rietveld, A., Sijens, P., Verkleij, A. J. & de Kruijff, B. (1983). Interaction of cytochrome *c* and its precursor apocytochrome *c* with various phospholipids. *EMBO J.* **2**, 907-913.
- Roder, H., Wagner, G. & Wüthrich, K. (1985). Amide proton exchange in proteins by EX1 kinetics: studies of basic pancreatic trypsin inhibitor at variable p<sup>2</sup>H and temperature. *Biochemistry*, **24**, 7396-7407.
- Roder, H., Elöve, G. A. & Englander, S. W. (1988). Structural characterisation of folding intermediates in

- cytochrome *c* by H-exchange labelling and proton NMR. *Nature*, **335**, 700-704.
- Sacchettini, J. C., Gordon, J. I. & Banaszak, L. J. (1988). The structure of crystalline *Escherichia coli*-derived rat intestinal fatty acid-binding at 2.5-Å resolution. *J. Biol. Chem.* **263**, 5815-5819.
- Speck, S. H., Neu, C. A., Swanson, M. S. & Margoliash, E. (1983). Role of phospholipid in the low affinity reaction between cytochrome *c* and cytochrome oxidase. *FEBS Letters*, **164**, 379-382.
- Spooner, P. J. R. & Watts, A. (1991). Reversible unfolding of cytochrome *c* upon interaction with cardiolipin bilayers. 1. Evidence from deuterium NMR measurements. *Biochemistry*, **30**, 3871-3879.
- van der Goot, F. G., González-Mañas, J. M., Lakey, J. H. & Pattus, F. (1991). A "molten-globule" membrane insertion intermediate of the pore-forming domain of colicin A. *Nature*, **354**, 408-410.
- Vik, S. B., Georgevich, G. & Capaldi, R. A. (1981). Diphosphadidylcholine is required for optimal activity of beef heart cytochrome *c* oxidase. *Proc. Natl Acad. Sci. USA*, **78**, 1456-1460.
- Wand, A. J., Roder, H. & Englander, S. W. (1986). Two-dimensional NMR studies of cytochrome *c*: hydrogen exchange in the N-terminal helix. *Biochemistry*, **25**, 1107-1114.
- Yi, Q. & Baker, D. (1996). Direct evidence for a two-state unfolding transition from hydrogen-deuterium exchange, mass spectrometry, and NMR. *Protein Sci.* **5**, 1060-1066.

*Edited by A. R. Fersht*

(Received 25 May 2000; received in revised form 14 September 2000; accepted 14 September 2000)